Journal of Mathematical Chemistry, Vol. 39, Nos. 3/4, May 2006 (© 2006)
DOI: 10.1007/s10910-005-9050-0

Hexagonite: A hypothetical organic zeolite

Michael J. Bucknum
Illinois Eastern Community College, 305 North West Street, Olney, IL 62450, USA

Eduardo A. Castro*
INIFTA, Suc. 4, C.C. 16, La Plata 1900, Argentina
E-mail: castro@quimica.unlp.edu.ar

Received 10 March 2005; revised 25 March 2005 / Published online: 13 January 2006

Elaborating the discrete hydrocarbon molecule bicyclo[2.2.2]-2,5,7-octatriene in three-dimensions, a unique, hypothetical allotrope of carbon is produced. Such a structure possesses a principal 6-fold axis; along this axis are hexagonal, organic tunnels with about a 5.70 Å outside tunnel diameter across opposite vertices, and an actual, inside diameter of 4.16 Å when taking into account the covalent radius of tetrahedral carbon. Across opposite edges, the outside hexagonal tunnel diameter is 4.94 Å, and the inside tunnel diameter is 3.61 Å. These tunnels are lined alternately with hexagonally disposed ethane-like functions and hexagonally disposed ethene-like functions that stack along the tunnel axis. The lattice lies in space group P6/mmm, and it has the Schläfli symbol given by $(6, 3^{2/5})$, it is therefore topologically related to the graphite–diamond hybrids. Because of the hexagonal symmetry of the unit cell, and also due to the fact that its polygonality is six, the structure has been given the name hexagonite. There are 10 carbon atoms in the unit of pattern, and the density is 2.50 g/cm^3; bordered by the densities of graphite at 2.27 g/cm^3 and diamond at 3.56 g/cm^3. Its large organic channels, lined with π organic functions, may make it particularly useful as an organic zeolite material, or alternatively as a host lattice for ionic conduction. The electronic band structure of the empty, hexagonal host lattice is described.

KEY WORDS: hexagonite, organic zeolite, crystal structure, organic tunnels

1. Introduction

The 3-,4-connected nets comprise a vast topological space of potential material crystal structures. Wells was the first crystallographer to systematically explore the 3-,4-connected nets [1]. Several crystal structures have been identified which are types of 3-,4-connected nets, including the Pt_3O_4 structure type, shown in figure 1, and the phenacite (Be_2SiO_4) structure type, shown in figure 2 [2,3].

* Corresponding author.

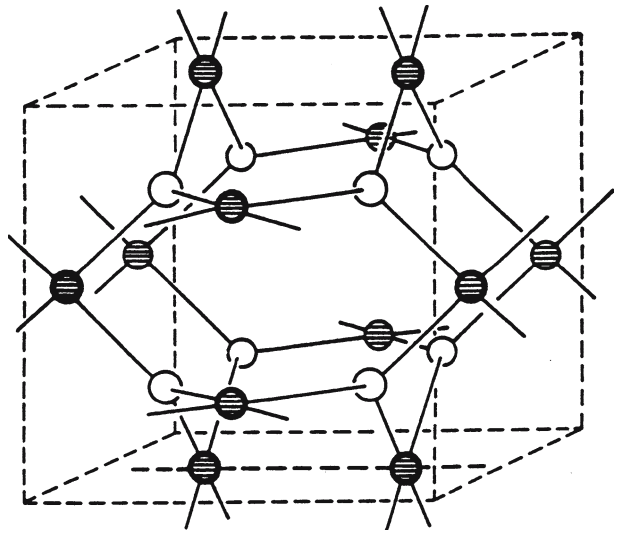

Figure 1. Crystal structure of the Pt_3O_4 lattice.

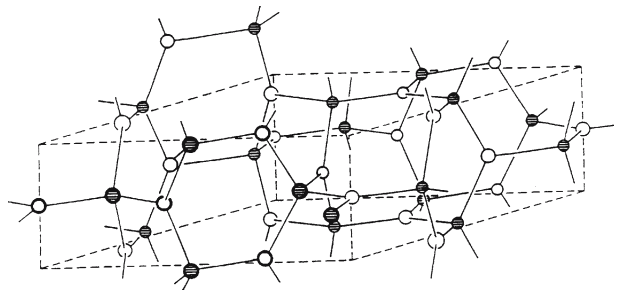

Figure 2. Crystal structure of the phenacite (Be_2SiO_4) lattice.

Theoretical studies of a C_3N_4 phase, adopting the phenacite structure type, indicate this material should have nearly the zero-pressure bulk modulus as that of the carbon diamond structure [4].

Previously, the crystal structure and electronic band structure of a novel 3-,4-connected carbon net was reported by us, and computation of its bulk modulus; both at zero-pressure, B_0, and at pressure, B, was carried out [5]. This hypothetical structure was shown to possess a higher bulk modulus than that of even the diamond structure. To construct this so-called "glitter" structure, one simply elaborates a three-dimensional structure from the discrete hydrocarbon molecule 1,4-cyclohexadiene [6]. The crystal structure of the glitter structure is shown in figure 3.

In the present report, a new and hypothetical 3-,4-connected network of carbon, and of the other p-block elements that adopt trigonal and tetrahedral

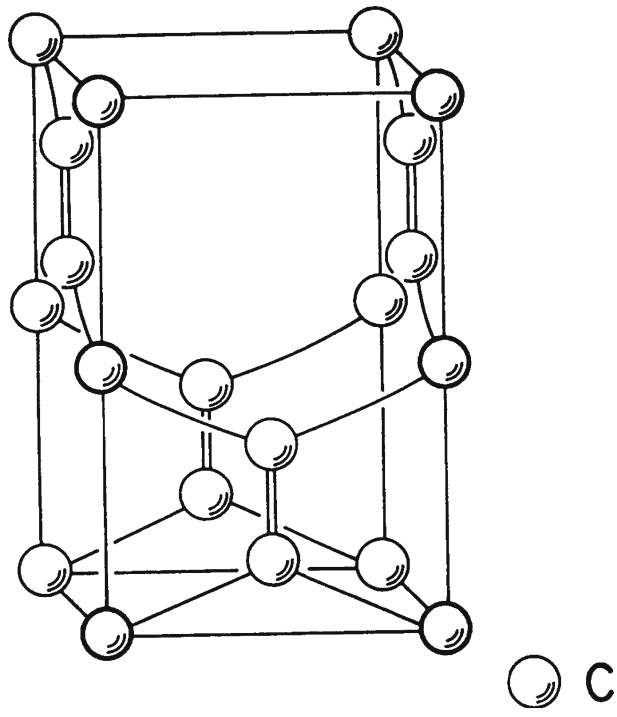

Figure 3. Crystal structure of the glitter lattice.

coordinations, like B, N, Al, Si and P, is described, This structure is produced by elaborating the molecule bicyclo[2.2.2]-2,5,7-octatriene (barrelene), shown in figure 4, in three-dimensions [7]. The unit of pattern of the material is hexagonal, in space group P6/mmm, number 191.[1] Figure 5 shows a view of an extended structure of this hexagonite structure, approximately inclined by 90° from the basal (*ab*-) plane.

It has 10 atoms in the unit cell, and a density of 2.50 g/cm^3. From a topological perspective, its Schläfli symbol, to be described in the following section, is given by (6, $3^{2/5}$).

The structure's most interesting feature are the large, hexagonal channels that run along its *c*-axis. These channels have a largest diameter, across opposite vertices of the hexagonal channel, of about 5.70 Å. This is the outside diameter of the channel, one must consider the actual covalent radius of carbon in computing a realistic inside, intercalation diameter for the hexagonal channels. The

[1] *International Tables for Crystallography*, Volume A, Space Group Symmetry (International Union of Crystallography, D. Reidel, Dordrecht, Holland, and Boston, 1983). The lattice has no glide planes or screw axes, and possesses a principal six-fold axis, vertical mirror planes, and horizontal mirror planes at $z = 0.305$ and 0.807.

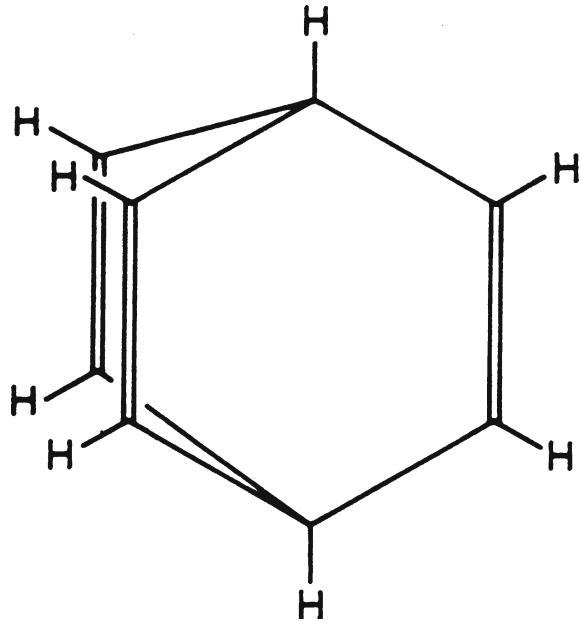

Figure 4. Structure of bicyclo[2.2.2]-2,5,7-octatriene.

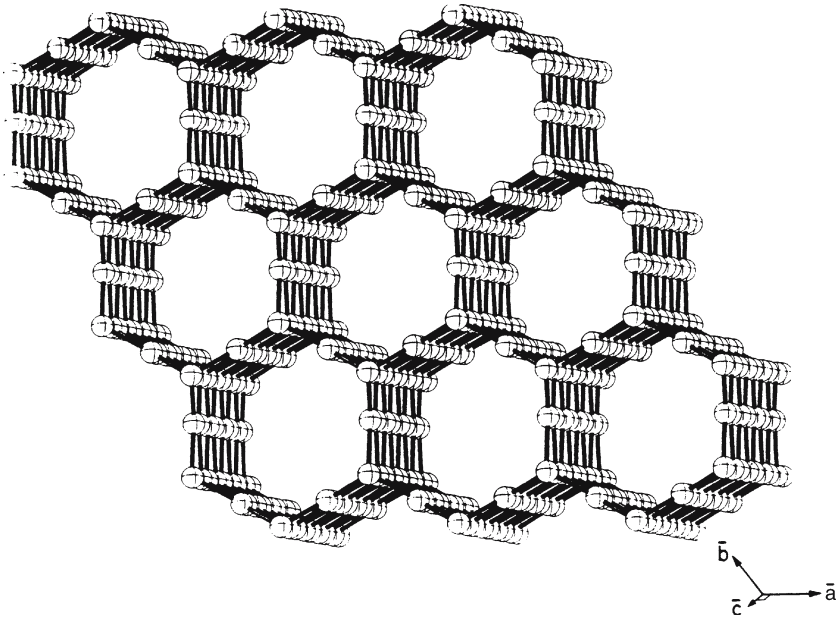

Figure 5. Extended drawing of the hexagonite lattice, viewed approximately normal to the *ab*-plane of the lattice.

covalent radius of tetrahedral carbon is 0.772 Å, yielding an actual inside diameter of 4.16 Å across opposite vertices of the hexagonal channel. Across opposite edges, the outside diameter is 4.94 Å, and the respective covalent radius of trigonal carbon is 0.667 Å, yielding an actual inside diameter across opposite edges of 3.61 Å [8]. Preliminary calculations are made as to the suitability for intercalating small organic and inorganic molecules inside the channels of hexagonite. Speculation is given of the ability of the π organic functions, lining the hexagonal channels, to catalytically reduce the oxides of carbon into methanol.

Approximate calculations of the band structure of hexagonite were made at the extended Hückel level of theory [9]. The electronic band structure and density of states (DOS) of the carbon phase is discussed in the final section. In the band structure, there are six π-type bands derived from the six p orbitals in the unit of pattern of hexagonite. Three of these bands are π bands and three are π^* bands. These six π-type bands border the Fermi level in the band structure of hexagonite. The DOS shows a relatively small band gap, which is attributed to the three π^* bands being relatively low-lying. It is therefore a semi-conductor, and an excellent candidate for doping with, for example, alkali metal atoms which could donate their lone s electron into the relatively low-lying π^* levels and transform the hexagonite structure into a π-type conductor [10].

2. Topology of the hexagonite structure

Euler's relation, shown in equation (1), marks the origin of the discipline of topology.[2] Here, the number of vertices, edges and faces of convex polyhedra are related into one unifying equation.

$$V - E + F = 2. \tag{1}$$

Other topological equations, related to equation (1), are possible. The polygonality of a convex polyhedron is given by the weighted average number of sides of the polygonal faces of a polyhedron, n. Similarly, the connectivity of a convex polyhedron, p, is given by the weighted average number of edges meeting at each vertex of a polyhedron. These indexes of a convex polyhedron, n and p, are termed its secondary topological indexes. From the identities shown in equations (2) and (3), relating the secondary topological indexes; the polygonality, n, and the connectivity, p, to the primary topological indexes, V, E and F; we may obtain another topological equation for the convex polyhedra.

$$nF = 2E. \tag{2}$$

$$pV = 2E. \tag{3}$$

[2] *Elementa doctrinae solidorum and Demonstratio nonnularum insignium proprietatum quibus solida heddris planis inclusa sunt praedita*, L. Euler, Proceedings of the St. Petersburg Academy, 1758.

Equation (2) simply states that because each edge joins two faces, the product of the weighted average polygonality (the number of edges, E, of each face, F) and the number of faces, is equal to $2E$. Similarly, because each edge terminates at two vertices, the product of the weighted average connectivity of the polyhedron and the number of vertices, V, is equal to twice the number of edges, E. By substituting these identities, shown in equations (2) and (3), into the Euler relation for the convex polyhedra, one may obtain the Schläfli relation shown as equation (4) [11].

$$\frac{1}{n} - \frac{1}{2} + \frac{1}{p} = \frac{1}{E}. \tag{4}$$

Unfortunately, the Schläfli relation has only rigorous solutions in terms of the convex polyhedra and polygons. Additionally, a one-dimensional pattern, a conventional polymer, can be thought of as an infinite polygon, so for these patterns, too, the Schläfli relation holds. However, for two- and three-dimensional patterns, like the graphite network and the diamond network, although one can rigorously determine the polygonality, n, and the connectivity, p, in the unit of pattern of these networks, the rigorous solution of the Schläfli relation for the number of edges, E, is not possible.

The secondary topological indexes, n and p, are characteristic of the polyhedra, polygons, and two- and three-dimensional networks. For an arbitrary crystal structure it may be difficult to assign links between the atoms unambiguously; in some cases, for example, it may be useful to view a crystal structure in terms of interpenetrating networks; but for the covalent materials such assignment is straightforward. These secondary topological indexes constitute the Schläfli symbols that characterize a material, (n, p). The ordered pairs of numbers can be used to construct a topology map of all structures. Table 1 shows a topology map for the "regular" structures.

Because the polygonality, n, and the connectivity, p, can be fractional for the polyhedra and two- and three-dimensional networks, the map shown in table 1 is only a partial map of all structures.

In the map are the familiar "regular" polyhedra; the tetrahedron, identified as, (3, 3), the cube (4, 3), the dodecahedron (5, 3), the octahedron (3, 4) and the icosahedron (3, 5). Vestiges of such objects play a prominent role in the structure of matter [12]. The emboldened border on the map separates the polyhedra and plane nets from the three-dimensional nets. This border is placed there to indicate that to its left the Schläfli symbol (n, p) represents a unique pattern of a discrete polyhedron or plane net. While to the right of the border, the three-dimensional nets, the Schläfli symbol (n, p) may indicate more than one way of producing a pattern that fills space.

Two interesting locations in the topology map in table 1, for the present report, are the entries (6, 3) and (6, 4). These represent the structures of graphite and diamond, respectively. By inspection of the graphite and diamond structures,

Table 1
A topology map of the regular structures.

	p						
n	3	4	5	6	7	8	...
3	*t*	*o*	*i*	(3, 6)	(3, 7)	(3, 8)	
4	*c*	(4, 4)	(4, 5)	(4, 6)	(4, 7)	(4, 8)	
5	*d*	(5, 4)	(5, 5)	(5, 6)	(5, 7)	(5, 8)	
6	(6, 3)	(6, 4)	(6, 5)	(6, 6)	(6, 7)	(6, 8)	
7	(7, 3)	(7, 4)	(7, 5)	(7, 6)	(7, 7)	(7, 8)	
8	(8, 3)	(8, 4)	(8, 5)	(8, 6)	(8, 7)	(8, 8)	
⋮							

shown in figures 6 and 7, one can clearly see the identities of the topological indexes, n and p.

Between (6, 3) and (6, 4) lie an infinite series of Catalán networks called the graphite–diamond hybrids. The word "Catalán" is derived from the Catalán polyhedra discovered in the 19th century [13]. Catalán polyhedra have fractional connectivity, p, and integer polygonality, n. Another, and dual, class of polyhedra are the Archimedean polyhedra, discovered by Archimedes in ancient Greece [13]. Buckminsterfullerene is a prominent example of an Archimedean polyhedron [14].

In 1994, the structure of the graphite–diamond hybrids was published [15]. Examples of this infinite series of structures are shown in figures 8 and 9. Their Schläfli symbol is given by $(6, 3^{x/y})$, where "x/y" is the ratio of four-connected

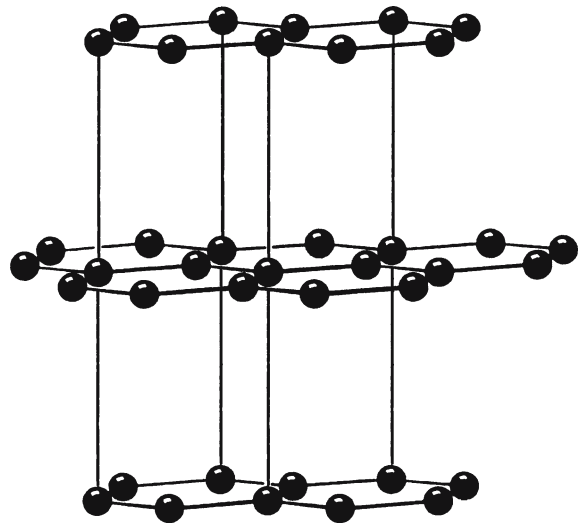

Figure 6. Crystal structure of the graphite lattice.

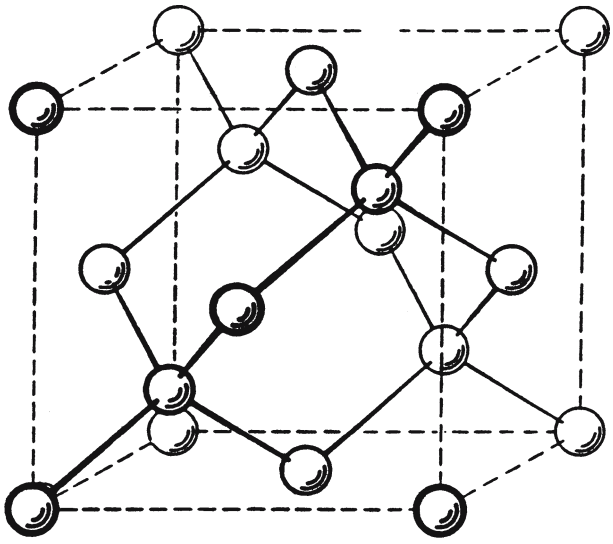

Figure 7. Crystal structure of the diamond lattice.

points in the unit of pattern to the number of points in the unit of pattern. The connectivity is a fractional number that runs between 3 (the graphite network) and 4 (the diamond network).

Technically, these Catalán networks are formed by fusing graphite sheets onto open valence tetrahedral connections (vertices) in various (hkl) planes of the diamond structure. The spacing between open valence tetrahedral connections in some (hkl) planes of the diamond structure is very closely matched to the width of the hexagons in the graphite structure, so it becomes possible to produce the graphite–diamond hybrids, from a purely hypothetical perspective, with little angular strain.

Among other things, the graphite–diamond hybrids are interesting from the point of view of their topology. From the construction of the hexagonite structure, it is clear that there is more than one way of filling space to obtain a Schläfli symbol resembling that of the graphite-diamond hybrids; $(6, 3^{x/y})$. From figure 10, a

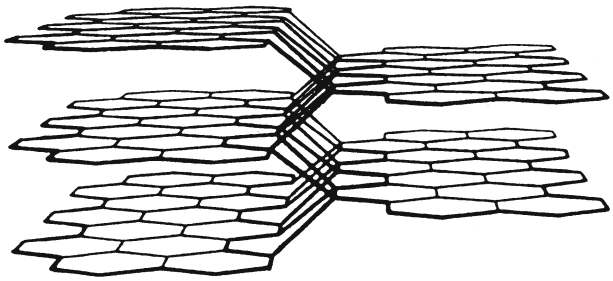

Figure 8. Structure of a variety of the "para-" graphite–diamond hybrids.

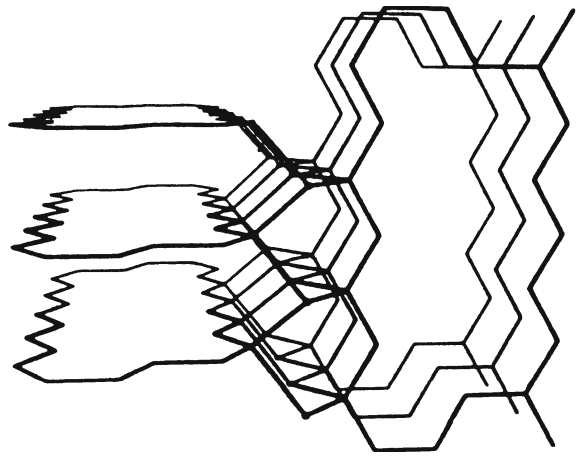

Figure 9. Structure of a variety of the "ortho-" graphite–diamond hybrids.

perspective of hexagonite in the *ab*-plane, it is obvious that all the shortest circuits about the three-, and four-connected, vertices in the unit of pattern are six-gons.

This is the case despite the large; the polygons in the hexagonal channels are twelve-gons, pores that run along the *c*-axis of the unit cell, since these are not shortest circuits about any of the vertices. The polygonality of hexagonite is therefore six. Of the 10 atoms in the unit of pattern of hexagonite, four of these atoms are tetrahedral and six of them are trigonal, therefore the connectivity, *p*, is 3.4. The Schläfli symbol of hexagonite, $(6, 3^{2/5})$, belongs to the Schläfli symbols for the infinite series of graphite–diamond hybrids, yet structurally it is not a graphite–diamond hybrid.

Finally, a recent paper has described possible three-dimensional carbon structures as progressive intermediates in the transformation of graphite to diamond [16]. This paper describes a computerized simulation of the contraction of the graphite structure in different crystallographic directions, including concomitant hybridization changes of carbon from sp^2 to sp^3, in some cases, followed by new bonding arrangements between "closing" carbon atoms. The paper is important, in the context of this communication, because in one of their figures (figure 3(c) in [16]) there is an intermediate structure of carbon which looks curiously analogous to the hexagonite structure.

3. Porosity of hexagonite

The calculations described in this report on hexagonite were performed by assuming a structure with all carbon–carbon single bonds of length 1.50 Å, all carbon–carbon double bonds of length 1.35 Å, and all bond angles; trigonal and tetrahedral, assumed to be 109.5°, except the axial trigonal bond angle which is constrained to 141°. With such parameters, a unit of pattern is obtained with

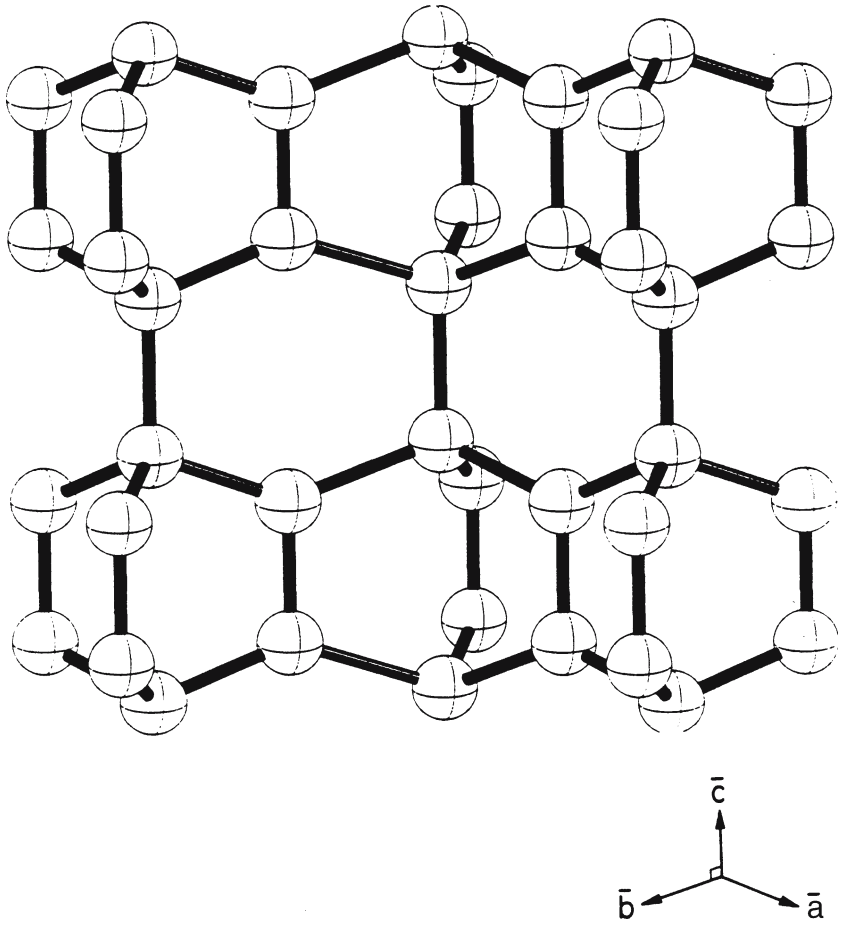

Figure 10. View of the hexagonite lattice from the perspective of the crystallographic *ab*-plane.

the lattice parameters; $a = 4.89$ Å, $b = 4.89$ Å, $c = 3.88$ Å, and $\alpha = 90°$, $\beta = 90°$ and $\gamma = 120°$. As previously mentioned, the density of hexagonite is 2.50 g/cm^3. In table 2 are indicated the rectilinear coordinates, in Å units, of the 10 atoms in the hexagonal (P6/mmm) unit cell of hexagonite. The origin of the unit cell coincides with one of its two 3-fold axes. A separate communication will describe the unit cell more completely.[3]

[3]D.C. Palmer, CrystalMaker Software, P.O. Box 183, Bicester, Oxfordshire, OX26 3TA, UK. Dr. Palmer has provided a compact description of the hexagonite unit cell. With the origin taken on one of the two 3-fold axes of the hexagonal unit cell, the asymmetric unit is given by two atoms in the following coordinates:

atom #	*x*/*a*	*y*/*b*	*z*/*c*
C1	0	0	0
C2	1/6	1/3	0.1300

Table 2
Rectilinear crystallographic coordinates of hexagonal (P6/mmm) hexagonite, in Å units.

atom #		x	*y*	*z*
1		0	0	0
2	(*a*-axis)	4.89	0	0
3	(*b*-axis)	−2.44	4.24	0
4	(*c*-axis)	0	0	3.88
5		0	1.41	0.513
6		0	2.82	0
7		−1.22	3.53	0.513
8		1.22	3.53	0.513
9		0	1.41	1.86
10		−1.22	3.53	1.86
11		1.22	3.53	1.86
12		0	2.82	2.38
13		0	0	2.38

Lattice parameters are $a = b = 4.89$ Å, $c = 3.88$ Å.

Figure 4 shows an extended view of the hexagonite structure, the perspective is approximately normal to the basal plane of the hexagonal unit cell. Evident in this picture is the two-dimensional array of hexagonal channels that form the essence of this structure. In this diagram, note the stacking of the hexagonally disposed trigonal atom pairs along the *c*-axis (tunnel axis) of the material. This is important from the perspective of catalysis, because these trigonal atom pairs, if made of carbon, add π organic functionality to the hexagonal channels. The π functions could act as donors of π electron density into the bonds of molecules which could be intercalated into the hexagonal channels.

The lateral dimensions of these channels are diagrammed in figure 11. As mentioned previously, the largest outside diameter, between oppositely disposed vertices of the channels, is 5.70 Å (inside diameter 4.16 Å). Opposite edges of the hexagonal channel, the separation between oppositely disposed π organic functions, is 4.94 Å (inside diameter 3.61 Å).

In comparison to actual mineral crystal structures of various conventional zeolites [17], the hexagonite channels are of intermediate size. For example, one of the smallest pore diameters of an actual zeolite is that found in sodalite, at a 2.50 Å pore diameter. At the other extreme, is a crystal structure which has proved exceptionally important for the "cracking" of heavier hydrocarbons in petroleum into the lighter hydrocarbons of gasoline, this is the mineral structure faujasite. Faujasite has a pore diameter of 8.00 Å. Therefore hexagonite, although not a conventional zeolite; being made of carbon, instead of the

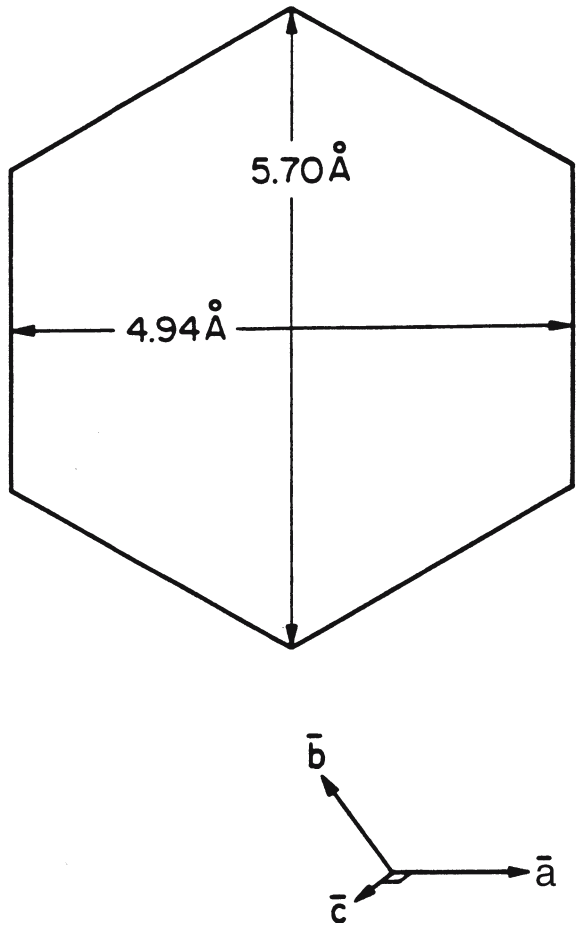

Figure 11. Lateral dimensions of the hexagonal hexagonite channels.

traditional silicon, aluminum and oxygen, still possesses pore diameters which compare with the intermediate-sized, traditional zeolites.[4]

These lateral dimensions of the hexagonal channels in hexagonite, make it suitable for the intercalation of small organic and inorganic molecules. Methane, with a tetrahedral edge of about 1.80 Å, would easily fit into the hexagonal pores of hexagonite. In addition, the water molecule, H_2O, with an intramolecular H-to-H distance of about 1.74 Å would also fit easily into the pores. Therefore one could, speculatively, envision processes such as the condensation reactions of methane to form the higher hydrocarbons, or the purification of water, assisted

[4]Traditional zeolites, either synthetic or naturally occurring, are defined as porous materials comprised of aluminum, silicon, oxygen and alkali metal or alkaline earth metal cations. The cations balance the charge of the tetrahedral aluminum–oxygen anions.

possibly by the π organic functionality lining the pores of hexagonite, as potential applications of this porous material [17, 18].

An important industrial reaction, the Fischer–Tropsch process, involves the reduction of carbon monoxide, CO, by hydrogen, H_2. A stoichiometric equation for this process is shown in equation (5) [18].

$$n\mathrm{CO} + (2n+1)\mathrm{H_2} \rightarrow \mathrm{C}_n\mathrm{H}_{2n+2} + n\mathrm{H_2O}. \tag{5}$$

The process occurs on a Co or Ni catalyst at close to room temperature. The CO molecule has a bond length of 1.13 Å and a diameter along this length of about 1.33 Å. With an inside, edge-to-edge diameter of 3.61 Å, carbon monoxide would easily fit into the hexagonal pores of hexagonite. Dihydrogen is the smallest molecule, its bond length is 0.74 Å, and it too would diffuse readily into hexagonite's pores.

Based upon a mechanism proposed in scheme 1 below, it is possible, albeit highly speculative, that a variation of the Fischer–Tropsch process, one involving only a partial reduction of CO to methanol, could be carried out in the hexagonal channels of hexagonite with the assistance of the adjacent π organic functions. Such a reaction is shown stoichiometrically, in equation (6).

$$\mathrm{CR_2} = \mathrm{CR_2} + 2\mathrm{H_2} + \mathrm{CO} \rightarrow \mathrm{CH_3OH} + \mathrm{CR_2} = \mathrm{CR_2}. \tag{6}$$

The scheme involves three fundamental steps, with the ethylene function on the channel wall operating as a catalyst. In the first step, the CO intercalated into the hexagonite channels coordinates to the ethylenic functions in the channel walls by forming a transient cyclopropanone-like complex. This step is called "carbon–oxygen bond activation". In the second step, a hydrogen molecule approaches the activated carbon–oxygen bond vertically (along the tunnel axis) and adds across the carbonyl function reducing the carbon–oxygen bond and forming a cyclopropanol-like complex coordinated to the hexagonite structure.[5] This second step is called the "reduction of the carbon–oxygen bond" step. Finally, in the last step, a hydrogen molecule approaches the coordinated alcohol; laterally in the *ab*-plane of the hexagonite structure, and terminates the weaker bonds of the cyclopropanol complex with stronger carbon-hydrogen bonds. In this third step, called the "termination" step, the cyclopropanol complex is transformed into a molecule of methanol as it adds the hydrogen molecule and simultaneously splits off from the hexagonite structure.

Such a transformation, the catalytic reduction of an oxide of carbon to methanol, would be of intense interest to those formulating a "renewable energy

[5]Strictly speaking, such a hydrogen addition reaction across a carbonyl function is thermally forbidden by symmetry analysis. Therefore, the proposed mechanism of methanol formation in Scheme 1 is highly speculative, and would depend upon the ethylene function of the hexagonite structure's wall "activating" the carbon–oxygen bond of the carbonyl towards reduction.

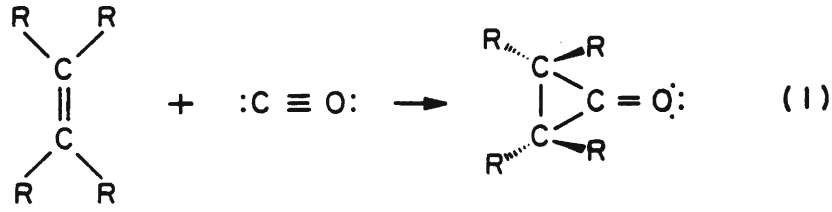

(1)

"carbon–oxygen bond activation"

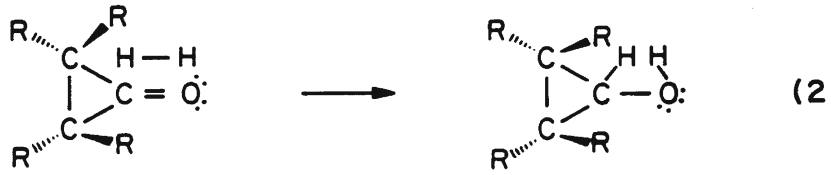

(2)

"reduction of carbon-oxygen bond"

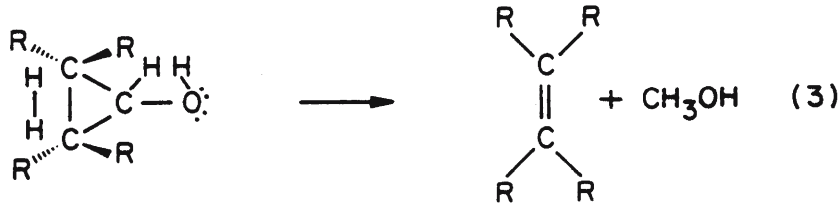

(3)

"termination and production of methanol"

economy" based upon the use of methanol as a fuel and as feedstock to the production of synthetic gasoline [19]. Obviously, the reduction of oxides of carbon to methanol would also have implications for the reduction of so-called "greenhouse gases" in the atmosphere; indeed one could envision the possibility of distilling off the oxides of carbon from liquefied air and using this as a source of methanol in conjunction with the catalytic properties of hexagonite discussed in this paper [19].

It appears that the limit of potential small molecules that could fit within hexagonite's pores would be benzene, C_6H_6. Hydrogens bonded on opposite sides of the benzene hexagon, "para" to each other, marked by "a" and "b" in figure 12, lie about 5.0 Å apart, this is the largest dimension of benzene [8].

Hydrogens lying "meta" to each other, indicated by positions marked "a" and "c" in figure 12, identify another characteristic width of the benzene hexagon, at about 4.3 Å. The thickness of the benzene hexagon, gotten from the covalent radius of trigonal carbon, is 1.33 Å [8]. Clearly, from these dimensions, benzene could not fit into the pores of hexagonite. Therefore, benzene would not be expected to diffuse into the hexagonite structure. One could, however,

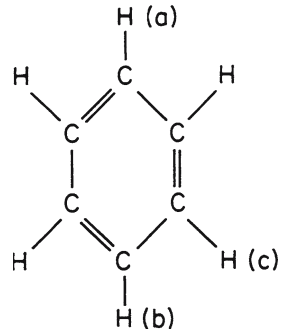

Figure 12. "Para" and "meta" positions in the benzene hexagon.

envision a "sila" derivative of hexagonite, in which all the tetrahedral carbons are replaced by silicon atoms. This structure would have the formula Si_2C_3. Such a structure might have a large enough inside pore diameter to accommodate benzene or substituted benzenes, like toluene.[6]

4. Electronic band structure of hexagonite

The electronic band structure and density of states (DOS) of the hexagonite structure has been calculated at the extended Hückel level of theory [9]. Figure 13 shows the band structure of hexagonite, and figure 14 shows the DOS of hexagonite.

There are 40 bands in the band structure of hexagonite, one for each of the four occupied orbitals of the 10 carbon atoms in the unit cell of the structure. What is particularly interesting in the band structure, are the levels bordering the Fermi energy; the dashed line across figure 14 at about −9.8 eV. These levels determine the external electronic structure of hexagonite. Figure 13 shows that there are 20 bands below the Fermi energy, the 20th band is just bordering this energy at about −9.8 eV. These are the bonding σ and π levels in the electronic

[6]Alternatively, it is possible to insert organic "spacers" into the hexagonite lattice in the form of 1,4-dimethylene-2,5-cyclohexadieneoid structural units. Such "spacers" would increase the number of atoms in the hexagonite unit cell and the lateral, *a*- and *b*-axes of the unit cell. Its possible that the six-fold axis could be lowered to one of two-fold symmetry (corresponding to an orthorhombic unit of pattern) by the asymmetrical insertion of these "spacer" units in the structure. For a symmetrical insertion of "spacer" units along the six edges of the hexagonal channels, the space group symmetry would remain P6/mmm. As one or more "spacer" units is inserted into the unit cell, the topology changes to (6, $3^{x/y}$), where "x" is the number of four-connected vertices in the unit cell (which will always be four) and "y" is the number of vertices in the unit cell (which will increase in size as more of the 1,4-dimethylene-2,5-cyclohexadieneoid, three-connected "spacers" are inserted along the hexagonal edges of hexagonite). The structure of such "expanded" hexagonite structures will be discussed in a separate communication.

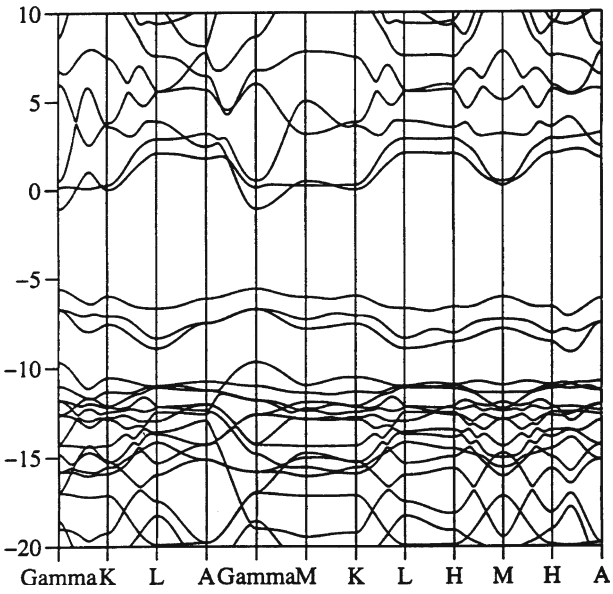

Figure 13. Electronic band structure of the hexagonite crystal structure.

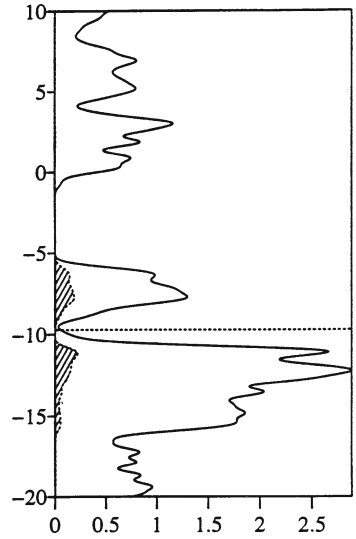

Figure 14. Density of states (DOS) of the hexagonite crystal structure.

structure of hexagonite. States just below, and above, the Fermi energy, in the so-called "valence band" and "conduction band", respectively, are derived from the six lone p orbitals in the unit cell of hexagonite. That this is so, is indicated by the shaded region in the DOS diagram, which is a projection of just one of the trigonal atom lone p orbitals in the DOS. There is a separation of about 1 eV

between π and π^* levels in hexagonite's electronic structure; therefore the material is a carbon-based semi-conductor.

Of the 20 anti-bonding levels in hexagonite, the three π^* levels are relatively low-lying. As can be seen in figure 13, these levels closely border the Fermi energy at -9.8 eV; separated from this energy by a small gap of approximately less than 1 eV. There is a relatively large gap between these three anti-bonding π^* levels, across the Brillouin zone, and the higher lying σ^* levels, which lie at, or above, 0 eV. Evidently, the σ^* levels play little, or no, role in the electronic structure of the material. The close proximity of the π and π^* states in the electronic structure of hexagonite; they are separated by less than 1 eV, suggests the possibility that this semi-conducting hexagonite structure could easily be doped with an alkali metal or alkaline earth metal that could donate its s electrons into the π^* levels of hexagonite and form a conducting system. The implications of such doping in terms of its potential use as an ionic conductor-host are not clear at this time [10,20].

Acknowledgments

Authors thank Norman Goldberg and Roald Hoffmann for their encouragement in the preparation of this paper. We also thank them for preparing the structural drawings of the hexagonite structure that were used in this paper. We thank Jane Jorgensen for her expert illustrations which were also used in this paper. We thank Henning Pape-Santos for his typesetting expertise used throughout this paper. Most especially one of us (MJB) thanks his wife, Hsi-cheng Shen, for giving loving support to him in this endeavour.

References

[1] A.F. Wells, The Geometrical Basis of Crystal Chemistry: (a) Part 1, A.F. Wells, Acta Cryst. 7 (1954) 535. (b) Part 2, A.F. Wells, Acta Cryst. 7 (1954) 545. (c) Part 3, A.F. Wells, Acta Cryst. 7 (1954) 842. (d) Part 4, A.F. Wells, Acta Cryst. 7 (1954) 849. (e) Part 5, A.F. Wells, Acta Cryst. 8 (1955) 32. (f) Part 6, A.F. Wells, Acta Cryst. 9 (1956) 23. (g) Part 7, A.F. Wells, and R.R. Sharpe, Acta Cryst. 16 (1963) 857. (h) Part 8, A.F. Wells, Acta Cryst. 18 (1965) 894. (i) Part 9, A.F. Wells, Acta Cryst. B24 (1968) 50. (j) Part 10, A.F. Wells, Acta Cryst. B25 (1969) 1711. (k) Part 11, A.F. Wells, Acta Cryst. B28 (1972) 711. (l) Part 12, A.F. Wells, Acta Cryst. B32 (1976) 2619. (aa) A.F. Wells, *Three Dimensional Nets and Polyhedra*, 1st edn. (1976) (John Wiley and Sons Inc., New York, 1977). (bb) A.F. Wells, *Further Studies of Three-dimensional Nets*, American Crystallographic Association, Monograph Number 8, 1st edn. (American Crystallographic Association Press, 1979).

[2] J. Waser and E.D. McClanahan, J. Chem. Phys. 19 (1951) 413.

[3] W.L. Bragg and W.H. Zachariasen, Zeit. f. Krist. 72 (1930) 518.

[4] A.Y. Liu and M.L. Cohen, Phys. Rev. B 41(15) (1990) 10727.

[5] (a) M.J. Bucknum and R. Hoffmann, J. Am. Chem. Soc. 116 (1994) 11456. (b) M.J. Bucknum, Carbon 35(1) (1997) 1. (c) M.J. Bucknum and E.A Castro, J. Math. Chem. 38 (1) (2005) 27.

[6] (a) L.A. Carreira, R.O. Carter and J.R. Durig, J. Chem. Phys. 59 (1973) 812. (b) H. Oberhammer and S.H. Bauer, J. Am. Chem. Soc. 91 (1969) 10. (c) G. Dallinga and L.H. Toneman, J. Mol. Structure 1 (1967) 117.
[7] (a) F.A. Cotton, *Chemical Applications of Group Theory*, 3rd edn. (John Wiley and Sons Inc., New York, 1990) p. 166. (b) H.E. Zimmerman and R.M. Paufler, J. Am. Chem. Soc. 82 (1960) 1514. (c) C.F. Wilcox, Jr., S. Winstein, and W.G. McMillan, J. Am. Chem. Soc. 82 (1960) 5450.
[8] L. Pauling, *The Nature of the Chemical Bond*, 3rd edn. (Cornell University Press, Ithaca, New York, 1960) p. 224.
[9] (a) R. Hoffmann, J. Chem. Phys. 39 (1963) 1397. (b) R. Hoffmann and W.N. Lipscomb, J. Chem. Phys. 37 (1962) 2872. (c) M.H. Whangbo and R. Hoffmann, J. Am. Chem. Soc. 100 (1978) 6093. (d) M.H. Whangbo, R. Hoffmann and R.B. Woodward, Proc. Roy. Soc. A 366 (1979) 23.
[10] (a) R.B. Kaner and A.G. MacDiarmid, Sci. Amer. 258 (1988) 60. (b) J.H. Burroughes, C.A. Jones and R.H. Friend, Nature 335 (1988) 137. (c) A.J. Epstein and J.S. Miller, Sci. Amer. 241 (1979) 48.
[11] M. Henle, *A Combinatorial Introduction to Topology*, 1st edn. (W.H. Freeman and Company, San Francisco, CA, 1979), p. 9.
[12] A.F. Wells, *Structural Inorganic Chemistry*, 5th edn. (Oxford University Press, New York, NY, 1984), Chapter 3.
[13] A.F. Wells, *Further Studies of Three-dimensional Nets*, American Crystallographic Association, Monograph Number 8, 1st edn. (American Crystallographic Association Press, 1979), p.3.
[14] H. Kroto, J.R. Heath, S.C. O'Brien, R.F. Curl and R.E. Smalley, Nature 318 (1985) 162.
[15] A.T. Balaban, D.J. Klein and C.A. Folden, Chem. Phys. Lett. 217 (1994) 266.
[16] J. Fayos, J. Solid State Chem. 148 (1999) 278.
[17] G.T. Kerr, Sci. Ameri. 259 (1989) 100.
[18] D.J. Cram and G.S. Hammond, *Organic Chemistry*, 2nd edn. (McGraw-Hill Book Company, New York, NY, 1964), p. 35.
[19] G. Olah, Chem. Eng. News 77(49) (1999) 121. These are personal comments given by Professor Olah in a millenium issue interview.
[20] D. Cram, Nature 356 (1992) 29.